JOURNAL OF SPACECRAFT AND ROCKETS
Vol. 32, No. 6, November–December 1995

Mars Pathfinder Six-Degree-of-Freedom Entry Analysis

Robert D. Braun,* Richard W. Powell,† Walter C. Engelund,* Peter A. Gnoffo,‡
K. James Weilmuenster,‡ and Robert A. Mitcheltree§
NASA Langley Research Center, Hampton, Virginia 23681

The Mars Pathfinder mission provides the next opportunity for scientific exploration of the surface of Mars following a 7.6 km/s direct entry. In support of this effort, a six-degree-of-freedom trajectory analysis and aerodynamic characteristic assessment are performed to demonstrate vehicle flyability and to quantify the effect that each of numerous uncertainties has upon the nominal mission profile. The entry vehicle is shown to be aerodynamically stable over a large portion of its atmospheric flight. Two low angle-of-attack static instabilities (freestream velocities of about 6.5 and 3.5 km/s) and a low angle-of-attack dynamic instability (supersonic) are identified and shown to cause bounded increases in vehicle attitude. The effects of center-of-gravity placement, entry attitude, vehicle roll rate, aerodynamic misprediction, and atmospheric uncertainty on the vehicle attitude profile and parachute deployment conditions are quantified. A Monte Carlo analysis is performed to statistically assess the combined impact of multiple off-nominal conditions on the nominal flight characteristics. These results suggest that there is a 99.7% probability that the peak attitude throughout the entry will be less than 8.5 deg, the peak heating attitude will be below 6.2 deg, and the attitude at parachute deployment will be less than 3.9 deg.

Nomenclature

b	= yaw/roll reference length, m
C_A	= axial force coefficient
C_D	= drag force coefficient
C_L	= lift force coefficient
C_m	= static pitching moment coefficient
$C_{m\alpha}$	= static stability parameter
C_{mq}	= dynamic pitch damping coefficient
C_N	= normal force coefficient
C_n	= static yawing moment coefficient
C_{nr}	= dynamic yaw damping coefficient
C_{pitch}	= total pitching moment coefficient
C_Y	= side force coefficient
C_{yaw}	= total yawing moment coefficient
c	= pitch reference length, m
I_{xx}, I_{yy}, I_{zz}	= moments of inertia in body axes, kg-m^2
L/D	= lift-to-drag ratio
M_m	= total pitching moment
M_n	= total yawing moment
q	= dynamic pressure, N/m^2
S	= reference aerodynamic area, m^2
V_e	= entry velocity, km/s
xcg, ycg, zcg	= c.g. position in body axes, m
xref, yref, zref	= aerodynamic reference point in body axes, m
α	= angle of attack, deg
α_T	= total angle-of-attack, $(\alpha^2 + \beta^2)^{1/2}$, deg
β	= sideslip angle, deg
γ_e	= entry flight-path angle, km/s

Presented as Paper 95-0456 at the AIAA 33rd Aerospace Sciences Meeting and Exhibit, Reno, NV, Jan. 9–12, 1995; received Jan. 18, 1995; revision received June 5, 1995; accepted for publication June 5, 1995.

*Aerospace Engineer, Space Systems and Concepts Division. Member AIAA.
†Senior Research Engineer, Space Systems and Concepts Division. Member AIAA.
‡Senior Research Engineer, Gas Dynamics Division. Associate Fellow AIAA.
§Aerospace Engineer, Gas Dynamics Division. Senior Member AIAA.

Introduction

THE Mars Pathfinder mission will provide the next opportunity for scientific exploration of Mars. The spacecraft is currently scheduled for launch in December 1996 onboard a Delta II rocket; Mars arrival is planned for July 1997. The entry vehicle contains a scientific instrument platform and microrover that are to be placed on the surface of Mars. In addition to its science mission, Mars Pathfinder is viewed as a proof-of-concept system needed to demonstrate the technology elements required for further exploration of Mars.[1–3]

Mission analysis and interplanetary trajectory tradeoffs for the Mars Pathfinder concept are summarized in Ref. 4. As sketched in Fig. 1, the Mars Pathfinder aeroshell[5] is based on its Viking predecessor, a 70-deg sphere-cone. However, vehicle geometry is essentially the only common entry characteristic between the two missions. As shown in Fig. 2, the Viking 1 and 2 entries were initiated from orbit (relative entry velocity of 4.5 km/s,[6–8] whereas the Pathfinder mission calls for a direct entry from its interplanetary flight path (relative entry velocity of 7.6 km/s).[4] Other entry characteristics for the two missions are summarized in Table 1. Mars Pathfinder is roughly half the mass and scale of the Viking entry vehicles. Additionally, the Viking entry vehicles utilized an active control system throughout their entries, making use of a center-of-gravity (c.g.) offset from the symmetry axis and reaction-control system propellant, to achieve flight at approximately 11-deg angle of attack.[7,8] Mars Pathfinder will not rely on any form of active

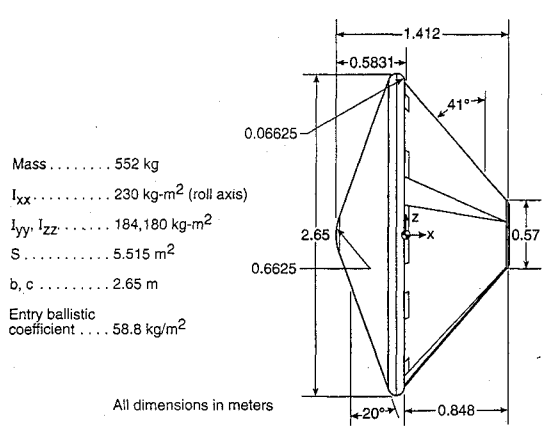

Fig. 1 Mars Pathfinder entry vehicle.

Table 1 Mars Pathfinder and Viking entry comparison

Entry characteristic	Mars Pathfinder	Viking
$V_{e,\text{inertial}}$, km/s	7.4[a]	4.73[a], 4.65[b]
$V_{e,\text{relative}}$, km/s	7.6 (retrograde)	4.50[a], 4.42[b] (direct)
$\gamma_{e,\text{relative}}$, deg	−14.8[a]	−17.63[b]
Entry mass, kg	552.0	980.8
S, m^2	5.52	9.62
α, deg	0.0	−11.1
C_D	1.7	1.6
Ballistic coefficient, kg/m^2	58.8	63.7
L/D	0.0	0.18
Guidance and control system	Spin stabilized	Three-axis control

[a]Measured at 125-km altitude. [b]Measured at 243.8-km altitude.

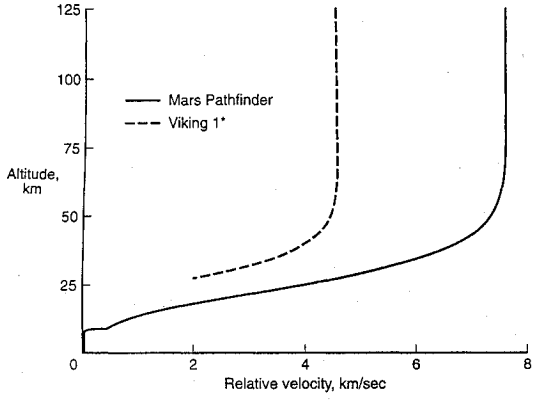

Fig. 2 Mars Pathfinder and Viking entry profile comparison.

control. Instead, mission planners are relying on an initial spin and aerodynamic damping to provide vehicle stability about the nominal 0-deg trim angle of attack, throughout the entire atmospheric flight.

In light of the differences between the Viking and Mars Pathfinder entry environment, a six-degree-of-freedom (DOF) aerodynamic characteristic assessment and trajectory analysis was performed. The primary objectives of these six-DOF analyses were to demonstrate the flyability of the Mars Pathfinder vehicle and to quantify the effect that each of numerous uncertainties (e.g., initial state errors, aerodynamic uncertainty, and mass property misprediction) had upon the nominal mission profile. In addition, these analyses have been used by the Mars Pathfinder project office to 1) address the effect that an initial vehicle wobble, incurred during the cruise-stage separation, would have upon the atmospheric flight, 2) quantify the impact of various uncertainties upon the parachute deployment conditions, 3) determine how close to the vehicle's axis of symmetry the c.g. should be located, and 4) provide information regarding the appropriate vehicle spin rate.

Before the flight of the Viking spacecraft, two distinct regions of aerodynamic instability had been noted by several investigators. In ballistic range tests through both air and CO_2 (the main constituent of the atmosphere of Mars), a static instability at small angles of attack was observed for the Viking aeroshell at Mach 7 (3.4 km/s).[9] Furthermore, a supersonic, dynamic instability at small angles of attack had been observed in several experimental (wind-tunnel and ballistic range) facilities.[10,11] Since the Mars Pathfinder vehicle is to fly without active control at a nominal 0 deg trim angle of attack, these instability results are of even more significance to this mission than during the Viking program. Therefore, another objective of the present analysis is to investigate the impact that such instabilities have on the Mars Pathfinder mission.

Analysis

Aerodynamics

The aerodynamic database utilized in the flight simulation studies was derived from a combination of computational fluid dynamics calculations, and wind-tunnel and ballistic range results. Aerodynamic predictions of the Mars Pathfinder lift, drag, and pitching moment characteristics were obtained from application of the high

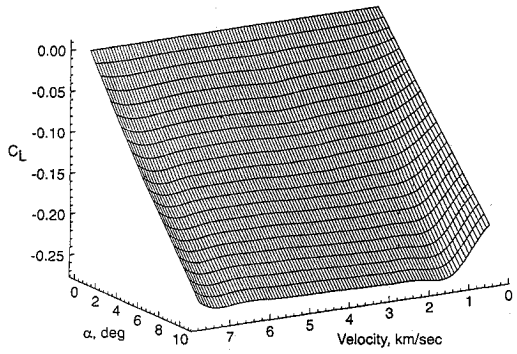

a) Lift coefficient vs velocity and angle of attack

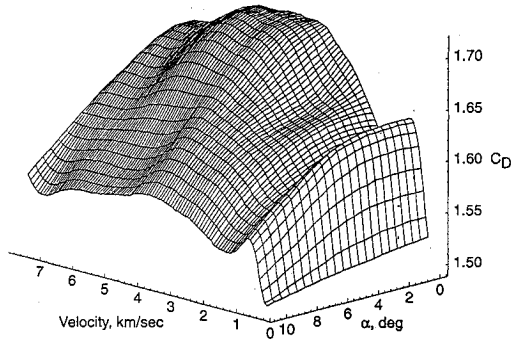

b) Drag coefficient vs velocity and angle of attack

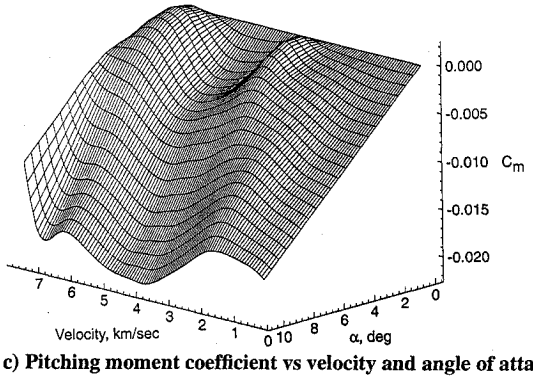

c) Pitching moment coefficient vs velocity and angle of attack

Fig. 3 Mars Pathfinder aerodynamic characteristics.

alpha inviscid solution (HALIS)[12] and Langley aerothermodynamic upwind relaxation algorithm (LAURA)[13] codes at numerous trajectory points over an angle of attack range of 0–11 deg. The Euler code, HALIS, was used to get an initial set of forebody aerodynamics in a timely manner. These inviscid results were supplemented with full-chemistry Navier–Stokes solutions obtained with LAURA. The LAURA program was explicitly written to solve three-dimensional, viscous, hypersonic flowfield problems in chemical and thermal nonequilibrium. The full set of aerodynamics was not obtained with LAURA due to the computational expense of each three-dimensional solution. However, excellent agreement between LAURA and HALIS aerodynamics estimates has been obtained in the past under aeroassisted flight experiment conditions (three-dimensional, thermochemical nonequilibrium, air).[14] Furthermore, the 11-deg angle-of-attack solutions obtained with the LAURA code showed excellent agreement with Viking flight data.[15] Base effects on C_D were calculated by including the afterbody in several of the full-chemistry Navier–Stokes solutions. The computed aerodynamic characteristics (C_L, C_D, C_m as a function of freestrem velocity and α) are shown in Figs. 3a–3c.

Based on the computational flowfield solutions, the static aerodynamic stability of the Mars Pathfinder aeroshell may be estimated. Figure 4 presents the static stability parameter $C_{m\alpha}$ as a function of angle of attack and velocity. Note that there are two distinct, low

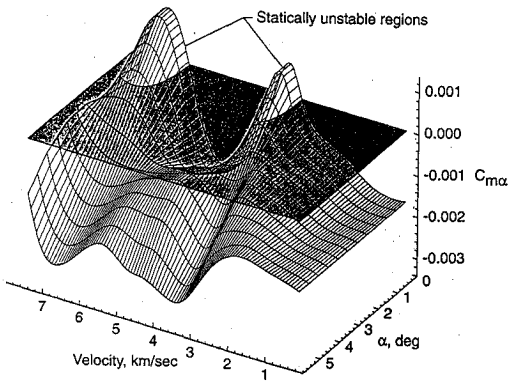

Fig. 4 Mars Pathfinder static stability.

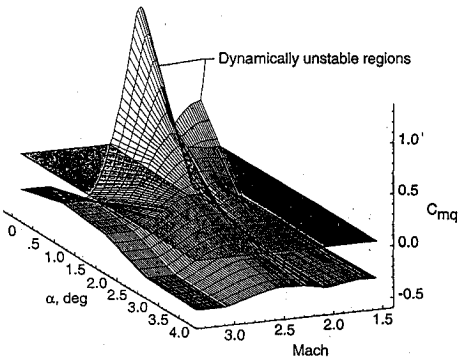

Fig. 5 Mars Pathfinder dynamic stability.

angle-of-attack regions of static instability, the first at about 6.5 km/s and the second at 3.5 km/s. In each of these regions, a small perturbation in the vehicle's angular orientation will result in an increasing vehicle attitude away from the trim state. This lack of static stability was predicted by both the HALIS and LAURA computational fluid dynamics analyses. Furthermore, the lower velocity instability is a perfect match to the phenomena predicted by NASA Ames ballistic range tests made during the Viking program.[9] These static instabilities are a result of an abrupt shift of the sonic line from the nose region to the shoulder on the windward side of the vehicle forebody under certain flowfield conditions.[15] Fortunately, both aerodynamic instabilities are confined to regions of low angle of attack. Hence, the increase in vehicle attitude caused by these phenomena will place the vehicle in a statically stable zone in which the attitude will be driven back towards the 0-deg trim state. In terms of mission significance, the high-velocity static instability is of more importance since this phenomenon occurs as the vehicle is near peak heating (discussed further in the "Results and Discussion" section).

Dynamic damping coefficients (C_{mq}) were taken directly from an extensive set of ballistic range and wind-tunnel measurements made in support of the Viking program.[16–18] Dynamic stability information could not be obtained computationally within the time constraints of the present analysis. Furthermore, because these data are difficult to obtain experimentally, the aerodynamic coefficients derived from the Viking preflight tests are subject to large measurement uncertainties. Figure 5 presents the dynamic stability parameter C_{mq} as a function of angle of attack and Mach number. As shown, the vehicle is dynamically stable for all angles of attack at Mach numbers above 2.5. Below Mach 2.5, the vehicle is dynamically unstable at low angles of attack. Hence, uncertainty in this parameter will mainly impact the parachute deployment conditions (nominally planned for Mach 1.8).

Based on the computational and experimental data presented in Figs. 3 and 5, a six-DOF aerodynamic database was constructed using a combination of linear and spline interpolation techniques. Eulerian rotations were used to obtain values of side force and yawing moment characteristics at nonzero sideslip conditions (making use of the vehicle's axisymmetry). Within the database, the aerodynamics are correlated by angle of attack, sideslip angle, and either

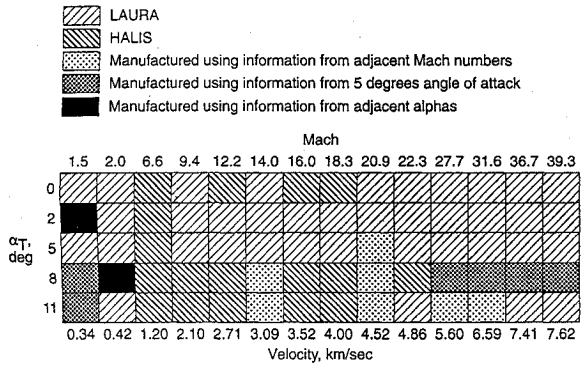

Fig. 6 Data sources used to assemble Mars Pathfinder static aerodynamic database.

velocity or Mach number (depending on the flight condition). The source of the static aerodynamic coefficients (Fig. 3 data) is illustrated in Fig. 6 for the various trajectory points. Note that for angles of attack of 5 deg and below, the static aerodynamics are mainly derived from the LAURA flowfield solutions. For a given flight condition and vehicle attitude, the database provides estimates (including base effects) of C_A, C_N, C_Y, C_m, C_n, C_{mq}, and C_{nr} for use in the six-DOF trajectory simulation. Note that a complete presentation of the Mars Pathfinder aerodynamic data is provided in Ref. 19.

Six-DOF Trajectory Simulation

The trajectory analysis was performed using the six-DOF version of the program to optimize simulated trajectories (POST).[20] This program has been utilized previously in a similar application.[21] In the present study, the program was utilized to integrate the six-DOF equations of motion from a given entry state to the parachute deployment conditions. The six-DOF aerodynamic database as well as Mars atmospheric and gravitational models were inputs to the simulation. In accordance with the Mars Pathfinder mission plans, no formal guidance and control strategy was used. A time-to-go algorithm that uses accelerometer measurements to estimate the time of parachute deployment was used to determine the trajectory termination point.[22] Note that this algorithm was derived from three-DOF flight simulation data assuming a 0-deg angle-of-attack flight; hence, six-DOF effects such as trim stability and the impact of lift and side forces have not been taken into account.

Summing the moments about the pitch and yaw axes, a coupled set of two nonlinear static trim equations were derived and added to the simulation:

$$\sum M_m = \left[C_m - C_A \left(\frac{zcg - zref}{c} \right) + C_N \left(\frac{xcg - xref}{c} \right) \right] qSc = C_{\text{pitch}} qSc$$

$$\sum M_n = \left[C_n - C_Y \left(\frac{xcg - xref}{b} \right) + C_A \left(\frac{ycg - yref}{b} \right) \right] qSb = C_{\text{yaw}} qSb$$

At a given point in the trajectory simulation, solution of these equations such that C_{pitch} and C_{yaw} equal zero yields the static trim attitude (α and β). Furthermore, for static stability,

$$\frac{\partial C_{\text{pitch}}}{\partial \alpha} < 0$$

$$\frac{\partial C_{\text{yaw}}}{\partial \beta} > 0$$

These static trim equations are not used in computing the six-DOF vehicle motion but were included to estimate the static vehicle

Table 2 Mars Pathfinder six-DOF entry analysis—nominal values and 3-σ uncertainities

	Nominal values	3-σ
C_L, C_Y	See Fig. 3a	±0.05
C_D above Mach 10	See Fig. 3b	±2%
C_D below Mach 5	See Fig. 3b	±10%
C_m, C_n above Mach 10	See Fig. 3c	±0.003
C_m, C_n below Mach 5	See Fig. 3c	±0.005
C_{mq}, C_{nr} above Mach 6	See Fig. 5	±21.6%
C_{mq}, C_{nr} above Mach 3	See Fig. 5	+110%, −48%
Entry flight-path angle, deg	−14.8	±1
C.G. offset along axis of symmetry, mm	583.1	±5
C.G. offset from axis of symmetry, mm	0.0	±5
Density above 100 km	Means Mars-GRAM	±60%
Density below 75 km	Means Mars-GRAM	±30%
Entry attitude, deg	0.0	±7
Entry yaw and pitch rates, deg/s	0.0	±1.1
Entry roll rate, deg/s	12.0	±0.6
Accelerometer measurement errors (two), m/s^2	0.0	±4.9
Timer errors (two), s	0.0	±0.25

trim attitude throughout the atmospheric flight. In this manner, a decomposition of the Mars Pathfinder motion into static and dynamic components is possible.

Numerous sources of uncertainty affect the Mars Pathfinder flight model. A portion of this uncertainty arises as a result of technology limitations (e.g., the interplanetary navigation system can only achieve the Mars entry state conditions to within a specified tolerance). A lack of knowledge concerning the Mars atmosphere and the computational uncertainty of the aerodynamics analysis are other contributing sources of error. Because the Mars Pathfinder configuration is currently undergoing detailed design, the center-of-gravity position is also subject to some change. Finally, entry attitude and attitude rate errors as a result of cruise-stage separation are possible. Therefore, in this analysis, an attempt was made to quantify and model the degree of uncertainty in each of 14 major parameters. The uncertainty range attributed to each of these parameters is listed in Table 2 along with the nominal values. For a parameter with more than one variance (e.g., drag coefficient or density), the uncertainty is estimated using linear interpolation between the two regions.

Results and Discussion

Nominal Mars Pathfinder Entry

The nominal Mars Pathfinder entry trajectory and attitude history are illustrated in Figs. 7 and 8. Note that throughout this investigation the vehicle attitude is denoted in terms of the total angle of attack α_T. This simplification is possible, without loss of generality, since the vehicle is axisymmetric. The nominal entry assumes no error in the entry interface attitude, c.g. placement, predicted atmospheric conditions, mass properties, or aerodynamics modeling.

As shown in Fig. 7, each of the atmospheric entries is initiated at 131 km with a relative entry velocity of 7.57 km/s. During flight, onboard accelerometers are used to sense a deceleration level of 5 g (about 51 s into the flight) and initiate a 10-s timer. At about this same time, the vehicle encounters the first static instability region as indicated by the abrupt increase in vehicle attitude shown in Fig. 8. This instability occurs as the vehicle is passing through peak heating (60 s). Another accelerometer measurement is taken 10 s after a deceleration level of 5 g is sensed. Based on this deceleration level, the onboard attitude information management system computes the time-to-go before parachute deployment. This timer is used to terminate each of the six-DOF entry trajectory simulations; in this case, the time-to-go is computed as 84.6 s, which corresponds to an entry time of 145.7 s. Also shown in Fig. 8, the vehicle flies through peak dynamic pressure (at about 70 s) with an associated increase in the oscillation frequency, the second static instability region (at about 77 s), which is evident by the second abrupt increase in vehicle attitude, and peak Reynolds number (about 80 s). Note that a final increase in attitude is seen as the vehicle flies below Mach 3, where it is dynamically unstable at low angles of attack.

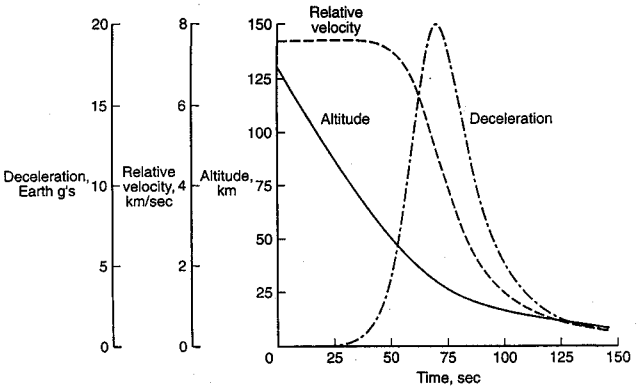

Fig. 7 Nominal six-DOF Mars Pathfinder entry trajectory characteristics.

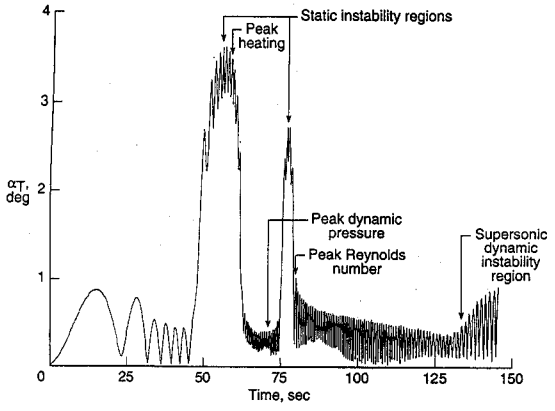

Fig. 8 Nominal six-DOF Mars Pathfinder entry attitude profile.

Note that even for the nominal case in which the vehicle enters with zero α and β (the static trim attitude for perfect c.g. placement), some small attitude oscillation is initially induced as the result of flight-path angle changes. Because the orientation of the relative velocity vector is not fixed, the vehicle develops an angle of attack and an oscillatory attitude motion about the trim state ensues.

Effect of Variations in the Major Parameters

To obtain further insight into the six-DOF atmospheric motion of the Mars Pathfinder vehicle, variations in the major parameters were examined independently. Where appropriate, the effects of multiple uncertainties were coupled. The major contributors to a dispersion in the entry vehicle's attitude history or parachute deploy conditions are summarized here.

Center-of-Gravity Placement

After assembly, the uncertainty in the spacecraft's c.g. should be quite small (with 1–2 mm). However, forcing the c.g. onto the vehicle's axis of symmetry requires additional mass to compensate for the payload's nonsymmetric mass distribution. If some angle of attack could be tolerated, a reduction in vehicle mass would be possible. Hence, the impact of c.g. offsets as large as 10 mm was investigated.

Significant movement of the c.g. along the symmetry axis (spacecraft's x axis, see Fig. 1) was possible without disturbing the vehicle's stability characteristics (or trim attitude). In fact, xcg variations as large as 250 mm were possible. The static trim attitude throughout the trajectory produced by various c.g. offsets away from the axis of symmetry is shown in Fig. 9. The effect of both static instability regions on trimmed attitude is evident. Note that a trim attitude above 5 deg in the peak heating region (6.5–6.6 km/s) will result for c.g. offsets greater than 5 mm. Figure 10 shows the vehicle attitude profile for a 3-mm c.g. offset from the axis of symmetry. In this case, entry begins with a 0-deg total angle of attack, but the vehicle aerodynamics cause an attitude reorientation such that oscillatory motion about the trim state (denoted by the dashed lines) is reached in about 30 s.

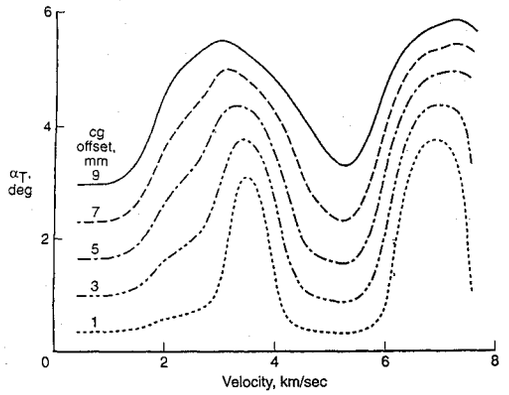

Fig. 9 Mars Pathfinder static trim attitude for various center-of-gravity offsets from the axis of symmetry.

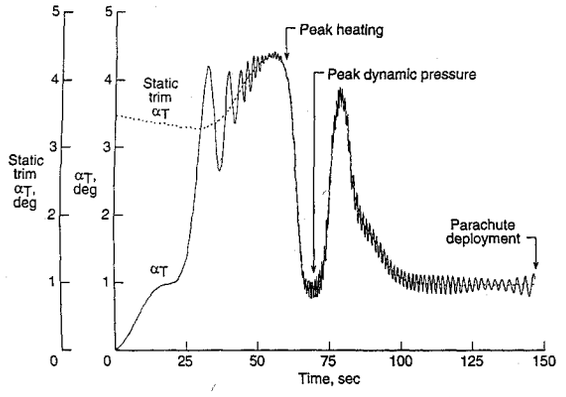

Fig. 10 Mars Pathfinder attitude profile for a 3-mm center-of-gravity offset from the axis of symmetry.

The general characteristics of the Mars Pathfinder attitude motion are also evident in Fig. 10. The trajectory is characterized by 1) an increase in vehicle attitude just before peak heating, 2) flight with a lower attitude, but higher oscillation frequency through peak dynamic pressure, 3) a second increase in vehicle attitude in the Mach 15–18 range (velocity of 3.2–3.8 km/s), and 4) a small increase in vehicle attitude as parachute deployment is reached. These entry attitude characteristics appear to some extent in all of the six-DOF trajectory simulations as a result of a lack of static or dynamic stability ($C_{m\alpha}$ and $C_{n\beta}$ or C_{mq} and C_{nr} effects) under certain flight conditions.

A c.g. offset from the symmetry axis also impacts the parachute deployment conditions as a result of small but nonnegligible lift and side forces. Without an adequate roll rate, the integrated effect of these forces can be quite large. For example, with a 5-mm c.g. offset, no initial roll rate, and no other uncertainties, variations of 12.9 km in parachute deployment altitude and of 1.62 in Mach number were noted. However, with a minimal roll rate (as low as 10 deg/s), the effect of these forces is substantially reduced to variances of 1.8 km in altitude and 0.21 in Mach number.

Atmospheric Interface Entry Attitude

As long as the c.g. is positioned relatively close to the symmetry axis (within a few millimeters), the vehicle will reorient itself from a different initial alpha and beta entry condition to an attitude motion consisting of a small oscillation about the static trim state during the first 50 s of entry. This level of aerodynamic stability is significant because the mission plans call for an attitude on the order of 5 deg or less through the peak heating region (typically 55–65 s from the entry interface). As demonstrated in Fig. 11, with the c.g. on the axis of symmetry, initial attitude errors as large as 9 deg are accommodated by the time the vehicle reaches the peak heating regime. As the c.g. offset from the symmetry axis increases, the time to damp towards the static trim attitude also increases slightly. However, by the time peak heating is reached, the attitude oscillations are generally within ±1.0 deg of the trim state (demonstrated in Fig. 10).

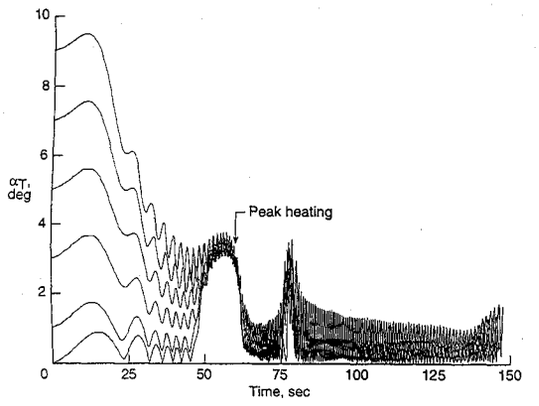

Fig. 11 Effect of initial attitude errors on Mars Pathfinder entry attitude profile.

These results imply that if the vehicle's c.g. can be located close enough to the axis of symmetry, the attitude correction propulsive maneuver currently in the Mars Pathfinder flight plan may not be necessary. This maneuver is currently in the mission profile to alter the vehicle's Earth-pointing attitude (an Earth-pointing attitude is maintained throughout the interplanetary flight) to a zero total angle-of-attack entry attitude. Removal of this attitude correction maneuver would provide simplification of the Mars Pathfinder mission plan and potentially lessen the risk. The results presented in Fig. 11 suggest that this maneuver may not be required because the aerodynamic moments (although small in magnitude) appear to provide enough damping to return the vehicle to its trim state from initial entry attitudes as large as 9 deg.

Vehicle Roll Rate

The vehicle roll rate must be chosen large enough such that any lift or side forces are nulled out by this spin but not so large that the induced inertial stability overwhelms the aerodynamic moments early in the flight. As discussed previously, this aerodynamic damping is needed early in the entry to reduce the effect of an initial attitude error and to reorient the vehicle as the flight-path angle changes. For too large of a roll rate, the gyroscopic stiffness produced through vehicle spin can overwhelm the aerodynamic moment and cause the vehicle to attempt to maintain an inertially fixed attitude. This situation is undesirable because an increasing angle of attack will result as the relative flight-path angle changes. On the other hand, without an adequate roll rate, the integrated effect of the lift and side forces on the parachute deploy conditions can be quite large. Fortunately, with a minimal roll rate (as low as 10 deg/s), the effect of these forces on the parachute deploy conditions is substantially reduced.

Viscous roll damping will occur during the trajectory as rotational energy is dissipated within the boundary layer. This phenomenon is well known for vehicles with large roll rates; however, for a vehicle spin on the order of 10–20 deg/s, this effect is difficult to quantify. Preliminary Navier–Stokes solutions (using the LAURA program) suggest that this effect will be small. For example, at peak dynamic pressure, where this viscous damping should be the largest, roll damping would induce an instantaneous 0.0338 deg/s change on a vehicle spinning at 12 deg/s. As a conservative estimate, one could assume that this torque is of constant magnitude for the entire 60-s dynamic pressure pulse. This approximation suggests a 2.03 deg/s decrease in the Mars Pathfinder roll rate (assuming an initial 12 deg/s spin). Note that the significance of this phenomenon will decrease as the vehicle roll rate and dynamic pressure decrease. As a result of these effects, a vehicle roll rate between 12 and 24 deg/s is suggested.

Drag Coefficient, Flight-Path Angle, and Atmospheric Density Variations

Variations in each of these parameters directly affect the ballistic flight path; hence, the aerothermodynamic environment and parachute deploy conditions will be altered from the nominal case. (The entry vehicle mass should also be included in this list; however, variations in this parameter as the design matures may be

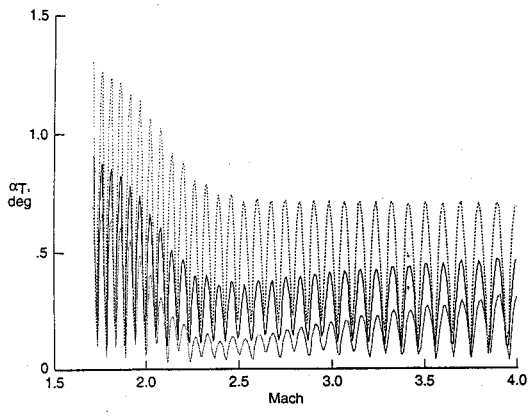

Fig. 12 Effect of dynamic stability uncertainty on parachute deployment attitude.

accommodated by a judicious selection of the nominal flight-path angle.) Assuming the 3-σ uncertainty levels listed in Table 2 for each of these three parameters, the parachute deployment altitude was found to range between 5.1–11.6 km, Mach number was between 1.5–2.1, and dynamic pressure was in the range 510–690 N/m^2.

Dynamic Stability Coefficients

As shown in Fig. 5, the Mars Pathfinder aeroshell is dynamically unstable at low angles of attack during supersonic flight. This prediction of instability is based on the ballistic range and wind-tunnel testing conducted before the flight of the Viking entry vehicles. Because these data are difficult to obtain experimentally, the aerodynamic coefficients derived from the Viking preflight tests are subject to large measurement uncertainties, as listed in Table 2.

As shown in Fig. 12, this uncertainty produces a factor of 2 variation in the potential attitude at parachute deployment. Note that the attitude profiles shown in Fig. 12 assume no c.g. offset and a roll rate of 12 deg/s. Although the degree of variation is roughly constant, larger attitudes are observed as the c.g. is moved away from the vehicle's axis of symmetry. Furthermore, because the attitude increases as the Mach number decreases, deploying the parachute at as high a Mach number as the other mission constraints will allow is suggested.

Multiple Off-Nominal Effects—Monte Carlo Analysis

During the actual flight of the Mars Pathfinder entry vehicle, some combination of off-nominal conditions will be encountered. Hence, it is important to statistically quantify each uncertainty such that the effect of the combinatorial variance of all of the parameters upon the nominal flight conditions may be assessed.[22] To accomplish this, each of the major parameters was modeled in a Gaussian sense based on the nominal and 3-σ uncertainty values listed in Table 2. Three thousand off-nominal cases were randomly estimated and simulated in a Monte Carlo manner. A 99.7% probability exists that each random parameter computed within the Monte Carlo analysis will be within the uncertainty bounds of Table 2. Vehicle attitude at several key trajectory points was monitored: 1) peak attitude throughout the entry, 2) peak heating attitude, 3) parachute deployment attitude, 4) attitude when the Reynolds number reaches $9.0e+05$ (estimated as the point where the forebody boundary layer could become turbulent), and 5) peak dynamic pressure attitude. Additionally, the parachute deployment conditions (time, altitude, dynamic pressure, and Mach number) were monitored.

The results of the six-DOF Monte Carlo simulations are graphically presented in Figs. 13–19 and tabulated in Table 3. In the distribution plots of Figs. 13–17, bins of 0.1 deg are shown. Note that each of these figures has the expected Gaussian shape with the exception of Fig. 13 that shows a bimodal distribution of peak attitude throughout the entry. This bimodal distribution is a result of peak attitude generally occurring in one of two distinct trajectory phases. If the initial attitude error is greater than about 5 deg, the peak attitude will occur in the first 10–20 s of flight. This large attitude will be damped early in the flight (before peak heating) and

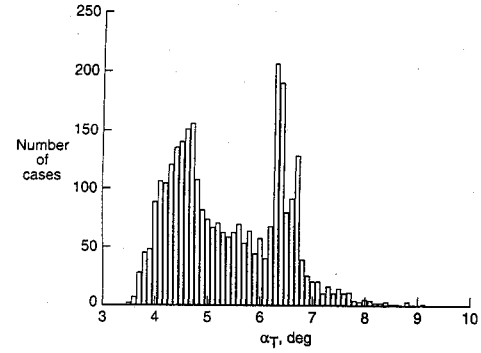

Fig. 13 Predicted peak attitude distribution from six-DOF Mars Pathfinder entry Monte Carlo analysis.

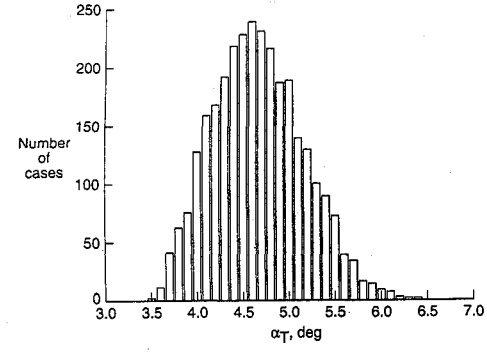

Fig. 14 Predicted peak heating attitude distribution from six-DOF Mars Pathfinder entry Monte Carlo analysis.

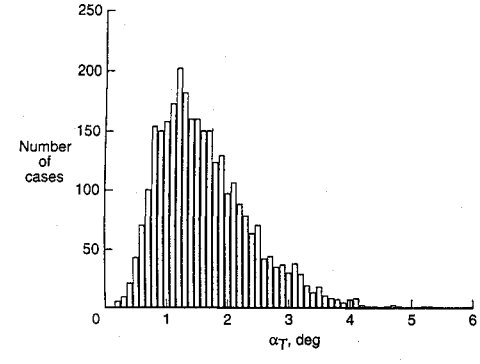

Fig. 15 Predicted parachute deployment attitude distribution from six-DOF Mars Pathfinder entry Monte Carlo analysis.

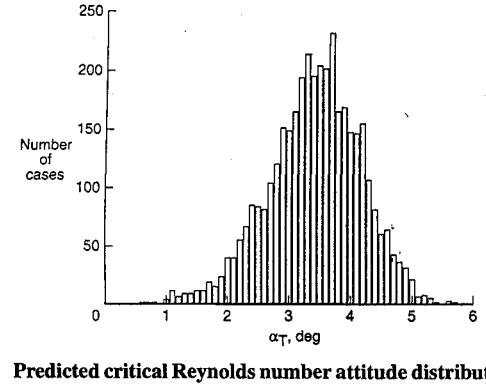

Fig. 16 Predicted critical Reynolds number attitude distribution from six-DOF Mars Pathfinder entry Monte Carlo analysis.

is the cause of the large number of cases between 6 and 7 deg in Fig. 13. When the initial attitude error is less than about 5 deg, the peak attitude will not occur until the first static instability region is reached (roughly coincident with peak heating). Hence, the other bimodal peak shown in Fig. 13 occurs at an angle of attack of about 4.5 deg, the same as the peak shown in Fig. 14.

Note that the mean peak attitude throughout the entry is 5.38 deg, mean attitude in the peak heating region is 4.67 deg, and the mean

Table 3 Six-DOF Mars Pathfinder entry Monte Carlo analysis statistics

	Mean value	Min.	Max.	1-σ
Maximum attitude throughout flight, deg	5.38	3.54	9.08	1.03
Peak heating attitude, deg	4.67	3.54	6.43	0.50
Parachute deployment attitude, deg	1.63	0.18	5.26	0.76
$Re = 9 \times 10^5$ attitude, deg	3.42	0.63	5.72	0.75
Peak dynamic pressure attitude, deg	1.21	0.25	4.33	0.55
Parachute deployment attitude, km	8.72	3.28	15.27	1.25
Parachute deployment Mach number	1.80	1.23	2.66	0.13
Parachute deployment dynamic pressure, N/m^2	596.8	436.7	757.8	36.83
Parachute deployment time, s	146.8	131.0	166.1	5.00

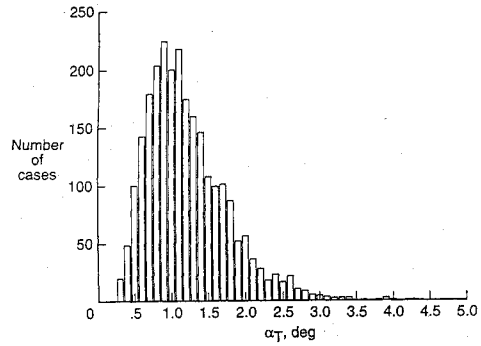

Fig. 17 Predicted peak dynamic pressure attitude distribution from six-DOF Mars Pathfinder entry Monte Carlo analysis.

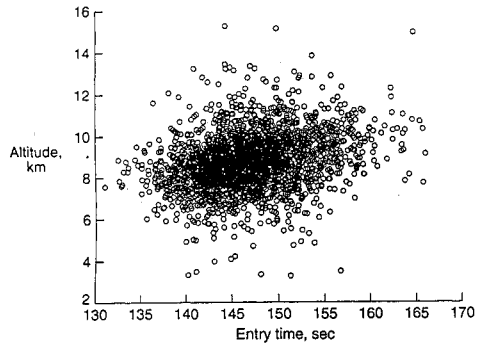

Fig. 18 Parachute deployment altitude and time-from-entry variation from six-DOF Mars Pathfinder entry Monte Carlo analysis.

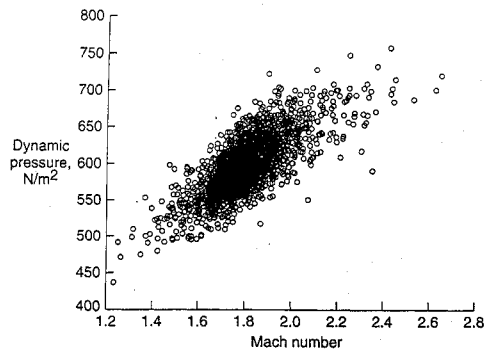

Fig. 19 Parachute deployment dynamic pressure and Mach number variation from six-DOF Mars Pathfinder entry Monte Carlo analysis.

attitude at parachute deployment is 1.63 deg. Maximum, minimum, and 1-σ variations on these values are presented in Table 3. The 1-σ variations should bound the parameter value in 68.3% of the cases. Hence, there is a 68.3% chance that the attitude at peak heating will be between 4.17 and 5.17 deg, a 95.4% chance that this attitude will be between 3.67 and 5.67 deg, and a 99.7% chance that this attitude will be between 3.17 and 6.17 deg. Similar statistical information may be derived from Table 3 for the other entry parameters listed.

Summary

The Mars Pathfinder mission will provide the next opportunity for scientific exploration of Mars. The science payload is to be placed on the surface of Mars following a 7.6 km/s direct entry from its interplanetary flight. During the atmospheric flight, mission planners are relying on the vehicle spin and aerodynamic damping to provide vehicle stability about the nominal 0-deg trim angle of attack. To demonstrate the flyability of the Mars Pathfinder aeroshell under the mission guidelines, a six-DOF trajectory analysis and aerodynamic characteristic assessment have been performed. Through this investigation, the vehicle aerodynamics and nominal six-DOF motion have been defined.

This analysis has shown that the Mars Pathfinder aeroshell is aerodynamically stable over a large portion of its atmospheric flight. Two low angle-of-attack static instabilities (about freestrem velocities of 6.5 and 3.5 km/s) and a low angle-of-attack dynamic instability (during supersonic flight) have been identified and shown to cause an increase in vehicle attitude. In each of these flight regimes, the vehicle is aerodynamically stable at higher angles of attack such that the increase in vehicle attitude is bounded. In general, the Mars Pathfinder attitude motion is characterized by 1) an increase in vehicle attitude just before peak heating, 2) flight with a lower attitude, but higher oscillation frequency through peak dynamic pressure, 3) a second increase in vehicle attitude just before peak Reynolds number that is quickly damped, and 4) a final increase in vehicle attitude as parachute deployment is reached.

The effects of center-of-gravity placement, entry attitude, vehicle roll rate, aerodynamic misprediction, and atmospheric uncertainty on the Mars Pathfinder attitude profile and parachute deployment conditions have also been addressed. A 5-mm center-of-gravity offset from the axis of symmetry is the maximum that can be tolerated if the attitude in the peak heating region is to be kept below 5 deg. Aerodynamic moments generated early in the entry were shown to provide enough damping to return the vehicle to its trim state from an initial attitude angle as large as 9 deg. The vehicle roll rate must be chosen large enough to account for viscous roll damping and to null out the effect of lift and side forces that will occur in flight. However, the roll rate must not be so large that the induced inertial stability overwhelms the aerodynamic moments early in the flight. As a compromise among these two conflicting requirements, a vehicle roll rate between 12 and 24 deg/s is suggested. Of all of the vehicle aerodynamics, the dynamic stability derivatives are known with the least certainty. This uncertainty was shown to produce a factor of 2 variation in the potential attitude at parachute deployment. To keep the parachute deployment attitude small, a small c.g. offset from the axis of symmetry is required. Furthermore, because the attitude increases as the Mach number decreases, deploying the parachute at as high a Mach number as the other mission constraints will allow is suggested.

A Monte Carlo analysis was performed to statistically assess the combined effect of multiple off-nominal conditions on the nominal flight path. These results suggest that there is a 99.7% probability that the peak attitude throughout the entry will be less than 8.5 deg, the peak heating attitude will be below 6.2 deg, and the attitude at parachute deployment will be less than 3.9 deg. Similar results are provided for the angular orientation at peak dynamic pressure and at a Reynolds number of $9.0e + 05$. The mean parachute deployment conditions were found to be an altitude of 8.72 km, Mach number of 1.8, dynamic pressure of 596.8 N/m^2, and an entry time of 146.8 s.

Acknowledgments

The authors are indebted to several members of the technical staff of the Jet Propulsion Laboratory, including D. Spencer, R. Cook, G. Singh, and K. Smith, for providing the atmospheric entry conditions, trajectory termination model, and several of the 3-σ uncertainty levels used in this analysis. Additionally, the assistance of P. Siemers of the NASA Langley Research Center concerning the Viking entry flight dynamics and preflight aerodynamic database has been appreciated.

References

[1]Bourke, R. D., Golombek, M. P., Spear, A. J., and Sturms, F. M., "MESUR and Its Role in an Evolutionary Mars Exploration Program," International Astronautical Federation, IAF Paper 92-0509, Aug. 1992.

[2]Lehman, D., Sutton, P., Sword, G. N., and McGee, D., "MESUR Technology Development," AIAA Paper 93-4191, Sept. 1993.

[3]Hubbard, G. S., Wercinski, P. F., Sarver, G. L., Hanel, R. P., and Ramos, R., "A Mars Environmental Survey (MESUR)—Feasibility of a Low Cost Global Approach," International Astronautical Federation, IAF Paper 91-432, Oct. 1991.

[4]Cook, R. A., and McNamee, J. B., "Mission Design for the Mars Environmental Survey," American Astronautical Society, AAS Paper 93-563, Aug. 1993.

[5]Tauber, M., Henline, W., Chargin, M., Papadopoulos, P., Chen, Y., Yang, L., and Hamm, K., "Mars Environmental Survey Probe Aerobrake Preliminary Design Study," *Journal of Spacecraft and Rockets*, Vol. 30, No. 4, 1993, pp. 431–437; see also AIAA Paper 92-2952, July 1992.

[6]Blanchard, R. C., and Walberg, G. D., "Determination of the Hypersonic-Continuum/Rarefied Flow Drag Coefficient of the Viking Lander Capsule 1 Aeroshell from Flight Data," NASA TP-1793, Dec. 1980.

[7]Anon., "Entry Data Analysis for Viking Landers 1 and 2, Final Report," Martin Marietta Corp., TN-3770218, Denver, CO, Nov. 1976; see also NASA CR 159388, Nov. 1976.

[8]Holmberg, N. A. Faust, R. P., and Holt, H. M., "Viking '75 Spacecraft Design and Test Summary, Volume I—Lander Design," NASA RP 1027, Nov. 1980.

[9]Intrieri, P. F., DeRose, C. E., and Kirk, D. B., "Flight Characteristics of Probes in the Atmospheres on Mars, Venus, and the Outer Planets," *Acta Astronautica*, Vol. 4, 1977, pp. 789–799; see also International Astronautical Federation, IAF Paper 76-076, Oct. 1976.

[10]Krumins, M. V., "Drag and Stability of Various Mars Entry Configurations," International Astronautical Federation, IAF Paper RE 138, Oct. 1968.

[11]Sammonds, R. I., and Kruse, R. L., "Viking Entry Vehicle Aerodynamics at $M = 2$ in Air and Some Preliminary Test Data for Flight in CO_2 at $M = 11$," NASA TN D-774, June 1975.

[12]Weilmuenster, K. J., and Hamilton, H. H., II, "Computed and Experimental Surface Pressure and Heating on 70-Deg Sphere Cones," *Journal of Spacecraft and Rockets*, Vol. 24, No. 5, 1987, pp. 385–393.

[13]Gnoffo, P. A., "Upwind-Biased, Point-Implicit Relaxation Strategies for Viscous, Hypersonic Flows," AIAA Paper 89-1972, June 1989.

[14]Weilmuenster, K. J., and Gnoffo, P. A., "Aeroassisted Flight Experiment Aerodynamic Characteristics at Flight Conditions," *Journal of Spacecraft and Rockets*, Vol. 27, No. 6, 1990, pp. 684–686.

[15]Gnoffo, P. A., Weilmuenster, K. J., Braun, R. D., and Cruz, C. I., "Effects of Sonic Line Transition on Aerothermodynamics of the Mars Pathfinder Probe," AIAA Paper 95-1825, June 1995.

[16]Anon., "Viking Aerodynamics Data Book," Martin Marietta Corp., TR-3709014, prepared under Contract NAS1-9000, Denver, CO, June 1972.

[17]Anon., "Experimental Pitch Damping Derivatives for Candidate Viking Entry Configurations at Mach Numbers from 0.6–3.0," Martin Marietta Corp., TR-3709005, prepared under Contract NAS1-9000, Denver, CO, June 1970.

[18]Uselton, B. L., Shadow, T. O., and Mansfield, A. C., "Damping-In-Pitch Derivatives of 120- and 140-deg Blunted Cones at Mach Numbers from 0.6 Through 3.0," ARO Inc., AEDC-TR-70-49, Arnold Air Force Station, TN, April 1970.

[19]Engelund, W. C., Gnoffo, P. A., Cruz, C. I., Braun, R. D., and Weilmuenster, K. J., "Aerodynamic Characteristics of the Mars Pathfinder Atmospheric Entry Configuration," NASA TM (in preparation).

[20]Brauer, G. L., Cornick, D. E., and Stevenson R., "Capabilities and Applications of the Program to Optimize Simulated Trajectories (POST)," NASA CR-2770, Feb. 1977.

[21]Powell, R. W., and Braun, R. D., "Six-Degree-of-Freedom Guidance and Control Analysis of Mars Aerocapture," *Journal of Guidance, Control, and Dynamics*, Vol. 16. No. 6, 1993, pp. 1038–1044.

[22]Spencer, D. A., and Braun, R. D., "Mars Pathfinder Entry Trajectory Design Using a Monte Carlo Approach," American Astronautical Society, AAS Paper 95-379, Aug. 1995.

K. J. Weilmuenster
Associate Editor